J|A|C|S
ARTICLES
Published on Web 01/31/2004

Determination of the Glycosidic Bond Angle χ in RNA from Cross-Correlated Relaxation of CH Dipolar Coupling and N Chemical Shift Anisotropy

Elke Duchardt,† Christian Richter, Oliver Ohlenschläger,‡ Matthias Görlach,‡ Jens Wöhnert, and Harald Schwalbe*

Contribution from the Institute for Organic Chemistry and Chemical Biology, Center for Biomolecular Magnetic Resonance, Johann Wolfgang Goethe-University Frankfurt, Marie-Curie-Strasse 11, D-60439 Frankfurt/Main, Germany

Received June 16, 2003; E-mail: schwalbe@nmr.uni-frankfurt.de

Abstract: A new heteronuclear NMR pulse sequence, the quantitative Γ(HCN) experiment, for the determination of the glycosidic torsion angle χ in $^{13}C,^{15}N$-labeled oligonucleotides is described. The Γ(HCN) experiment allows measurement of CH dipole−dipole, N chemical shift anisotropy cross-correlated relaxation rates ($\Gamma^{DD,CSA}_{C1'H1',N1}$ and $\Gamma^{DD,CSA}_{C2'H2',N1}$ for pyrimidines and $\Gamma^{DD,CSA}_{C1'H1',N9}$ and $\Gamma^{DD,CSA}_{C2'H2',N9}$ for purines). A nucleotide-specific parametrization for the dependence of these Γ-rates on χ based on ^{15}N chemical shift tensors determined by solid-state NMR experiments on mononucleosides (Stueber, D.; Grant, D. M. *J. Am. Chem. Soc.* **2002**, *124*, 10539−10551) is presented. For a 14-mer and a 30-mer RNA of known structures, it is found that the Γ(HCN) experiment offers a very sensitive parameter for changes in the angle χ and allows restraining of χ with an accuracy of around 10 degrees for residues which do not undergo conformational averaging. Therefore, the Γ(HCN) experiment can be used for the determination of χ in addition to data derived from ^3J(C,H)-coupling constants. As shown for the 30-mer RNA, the derived torsion angle information can be incorporated as additional restraint, improving RNA structure calculations.

Introduction

Since the investigation of RNA by multidimensional heteronuclear NMR methods was made possible due to the development of techniques for the preparation of ^{13}C and ^{15}N isotope labeled RNA in 1992,[1−4] a large number of NMR experiments have been devised[5,6] aimed at improving the accuracy of NMR-derived RNA structures. Among the still less well-characterized torsion angles in RNA is the glycosidic bond angle χ, which defines the orientation of the aromatic bases with respect to the ribose moiety (Figure 1). χ is sterically restricted to either the *anti* ($\chi \approx 240°$) or the *syn* ($\chi \approx 60°$) conformation. By NMR, χ can be determined from the intensity of the H1′−H6 (pyrimidines) or H1′−H8 (purines) cross-peaks in a NOESY spectrum with an accuracy of about ±50°,[7] resulting in a qualitative discrimination between the *syn* and the *anti* conformation. A more accurate determination of χ can be achieved either from a more detailed NOE analysis including the H2′−H6/8 and H3′−H6/8 NOEs[7] or from the interpretation of ^3J(C2/C4,H1′)- and ^3J(C6/C8,H1′)-coupling constants.[8−10] However, NOE distance information is not very precise due to various effects such as spin diffusion. Furthermore, the accuracy of angle determination based on the analysis of heteronuclear coupling constants depends on the quality of the underlying Karplus parametrization. Recently, refined Karplus equations have been provided for ^3J(C2,H1′), ^3J(C4,H1′), ^3J(C6,H1′), and ^3J(C8,H1′) in the different nucleotides of DNA.[10] However, the validity of these equations for RNA still remains to be investigated. In addition, coupling constant determination is prone to systematic errors for larger molecules.[8,9]

Apart from coupling constants, cross-correlated relaxation rates (Γ-rates) can be exploited to obtain angular information by virtue of their dependence on the relative orientation of two spatially directed properties, which can in turn be related to the molecular frame. Γ-rates have only recently been introduced as novel NMR restraints for structure determination in solution[11] and have since found widespread application for the measurement of different torsion angles in proteins, oligonucleotides, and carbohydrates.[12−20]

† Additional affiliation: Massachusetts Institute of Technology, Department of Chemistry, 77 Massachusetts Avenue, Cambridge, MA 02139.

‡ Institute of Molecular Biotechnology (IMB), Department of Molecular Biophysics/NMR Spectroscopy, Beutenbergstrasse 11, D-07745 Jena, Germany.

(1) Batey, R. T.; Inada, M.; Kujawinski, E.; Puglisi, J. D.; Williamson, J. R. *Nucleic Acids Res.* **1992**, *20*, 4515−4523.
(2) Batey, R. T.; Battiste, J. L.; Williamson, J. R. *Methods Enzymol.* **1995**, *261*, 300−322.
(3) Nikonowicz, E. P.; Sirr, A.; Legault, P.; Jucker, F. M.; Baer, L. M.; Pardi, A. *Nucleic Acids Res.* **1992**, *20*, 4507−4513.
(4) Varani, G.; Aboul-ela, F.; Allain, F. H.-T. *Prog. Nucl. Magn. Reson. Spectrosc.* **1996**, *29*, 51−127.
(5) Varani, G.; Tinoco, I., Jr. *Q. Rev. Biophys.* **1991**, *24*, 479−532.
(6) Cromsigt, J.; van Buuren, B.; Schleucher, J.; Wijmenga, S. S. *Methods Enzymol.* **2001**, *338*, 371−399.
(7) Wijmenga, S. S.; Mooren, M. M. W.; Hilbers, C. W. *NMR of Macromolecules*; Oxford University Press: New York, 1995; pp 217−288.
(8) Schwalbe, H.; Marino, J. P.; King, G. C.; Wechselberger, R.; Bermel, W.; Griesinger, C. *J. Biomol. NMR* **1994**, *4*, 631−644.
(9) Trantirek, L.; Stefl, R.; Masse, J. E.; Feigon, J.; Sklenar, V. *J. Biomol. NMR* **2002**, *23*, 1−12.
(10) Munzarova, M.; Sklenar, V. *J. Am. Chem. Soc.* **2003**, *125*, 3649−3658.
(11) Reif, B.; Hennig, M.; Griesinger, C. *Science* **1997**, *276*, 1230−1233.

10.1021/ja0367041 CCC: $27.50

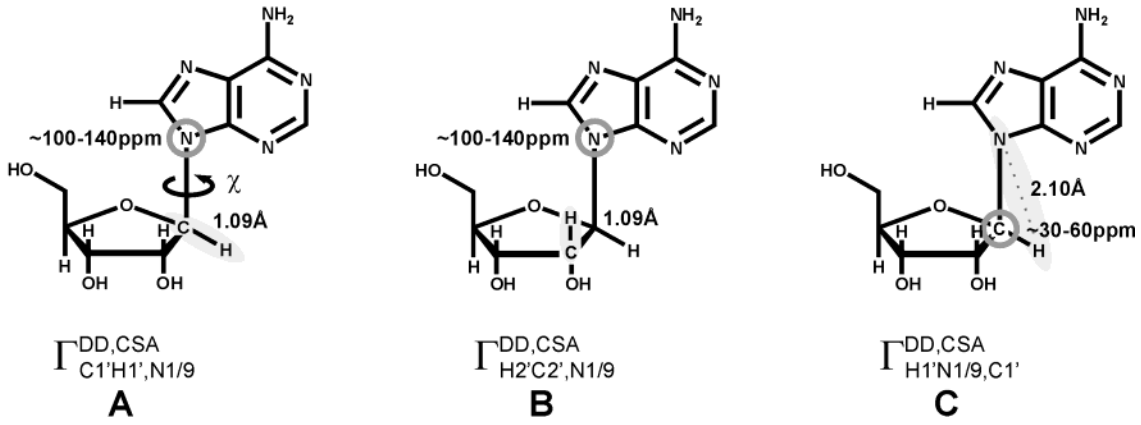

Figure 1. Schematic representation of $\Gamma^{DD,CSA}_{C1'H1',N1/9}$ (A), $\Gamma^{DD,CSA}_{H2'C2',N1/9}$ (B), and $\Gamma^{DD,CSA}_{H1'N1/9,C1'}$ (C) in the molecular frame of adenosine. The lengths of the interatomic vectors and the approximate sizes of the chemical shift anisotropies are given.

In this report, we have investigated the use of $\Gamma^{DD,CSA}_{C1'H1',N1/9}$, the cross-correlated relaxation rate between the C1′H1′ dipole−dipole vector and the chemical shift tensor (CS-tensor) of N1 (pyrimidines) or N9 (purines) in the glycosidic linkage of RNA (or DNA), for the determination of χ (Figure 1A).

The interpretation of $\Gamma^{DD,CSA}_{C1'H1',N1/9}$ requires a χ-dependent parametrization, which relies on knowledge of the N1 and N9 CS-tensors. CS-tensors derived from model compounds in the solid state or from ab initio calculations have to be used under the simplifying assumption that any conformational dependence can be disregarded. Furthermore, apart from providing structural information, cross-correlated relaxation rates are sensitive to motional molecular properties such as the extent of overall as well as internal motion and motional anisotropy. The latter is particularly important for nucleic acids, which exhibit a large extent of anisotropy even for relatively small molecules.

Recently, an experiment for the determination of dipole−dipole, CSA cross-correlated relaxation rates in the glycosidic linkage of RNA has been reported, together with a detailed dynamical treatment for one reference structure.[21] This analysis included the effects of internal motion as well as anisotropic diffusion, assuming that the diffusion tensor (and its appearance in a water shell) can be taken as a reliable model for the rotational tensor.

Here, we took a different approach in that we aimed at investigating $\Gamma^{DD,CSA}_{C1'H1',N1/9}$ as a *ready-to-use* structural parameter with an uncomplicated angle extraction process comparable to the one for ^3J-coupling constants. Therefore, we explored a simplified parametrization for $\Gamma(\chi)$ using an isotropic model of rotational tumbling together with conformational rigidity. ^{15}N CS-tensor values and orientations derived on mononucleosides in the solid state[22] were used. The investigation comprised two RNA model molecules of different sizes (a 14-mer and a 30-mer) but similar secondary structure (Figure 2).

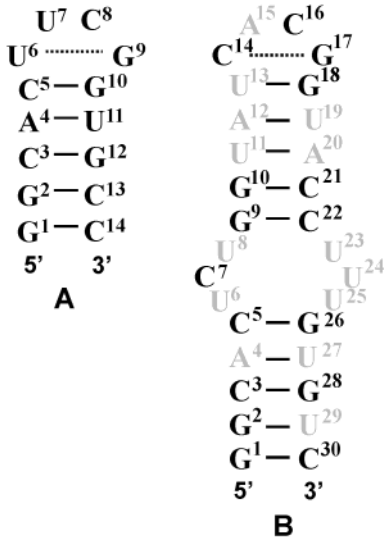

Figure 2. Secondary structures of the 14-mer (A) and the 30-mer (B) RNA investigated in this report. The 14-mer is fully ^{13}C,^{15}N-labeled, the 30-mer is only labeled in the cytosine and the guanosine residues, which are shown in black.

Investigation of the 14-mer, which is almost isotropic, and the more anisotropic 30-mer RNA serves the twofold purpose of examining both the influence of the simplifying assumptions and the applicability of the new experiment to larger molecules with less favorable relaxation behavior. To assess the quality of this new method, we compared our data to the currently available torsion angle determination method from ^3J(C,H)-coupling constants.[10] In addition, we introduce $\Gamma^{DD,CSA}_{C2'H2',N1/9}$ (Figure 1B) as an additional parameter serving to decrease the inherent degeneracy of $\Gamma(\chi)$ in favorable cases.

Theoretical Background

In the simple case of isotropic molecular motion and isotropic fast time-scale internal motion, $\Gamma^{DD,CSA}_{C1'H1',N1/9}$ is given by (eq 1):

$$\Gamma^{DD,CSA}_{C1'H1',N1/9} = -\frac{2}{15}\frac{\mu_0}{4\pi}\frac{\omega_N\gamma_C\gamma_H}{r_{C1'H1'}{}^3}\hbar S^2_{C1'H1',N1/9}\tau_c * [\sigma^N_{11}(3\cos^2\theta^{C1'H1',N1/9}_{11} - 1) + \sigma^N_{22}(3\cos^2\theta^{C1'H1',N1/9}_{22} - 1) + \sigma^N_{33}(3\cos^2\theta^{C1'H1',N1/9}_{33} - 1)] \quad (1)$$

(12) Schwalbe, H.; Carlomagno, T.; Hennig, M.; Junker, J.; Reif, B.; Richter, C.; Griesinger, C. *Methods Enzymol.* **2001**, *338*, 35−81.
(13) Carlomagno, T.; Blommers, M. J.; Meiler, J.; Cuenoud, B.; Griesinger, C. *J. Am. Chem. Soc.* **2001**, *123*, 7364−7370.
(14) Boisbouvier, J.; Bax, A. *J. Am. Chem. Soc.* **2002**, *124*, 11038−11045.
(15) Riek, R. *J. Magn. Reson.* **2001**, *149*, 149−153.
(16) Bertini, I.; Kowalewski, J.; Luchinat, C.; Parigi, G. *J. Magn. Reson.* **2001**, *152*, 103−108.
(17) Banci, L.; Bertini, I.; Felli, I. C.; Hajieva, P.; Viezzoli, M. S. *J. Biomol. NMR* **2001**, *20*, 1−10.
(18) Vincent, S. J. F.; Zwahlen, C. *J. Am. Chem. Soc.* **2000**, *122*, 8307−8308.
(19) Zwahlen, C.; Vincent, S. J. F. *J. Am. Chem. Soc.* **2002**, *124*, 7235−7239.
(20) Ilin, S.; Bosques, C.; Turner, C.; Schwalbe, H. *Angew. Chem.* **2003**, *115*, 1394−1397.
(21) Ravindranathan, S.; Kim, C.-H.; Bodenhausen G. *J. Biomol. NMR* **2003**, *27*, 365−375.
(22) Stueber, D.; Grant, D. M. *J. Am. Chem. Soc.* **2002**, *124*, 10539−10551.

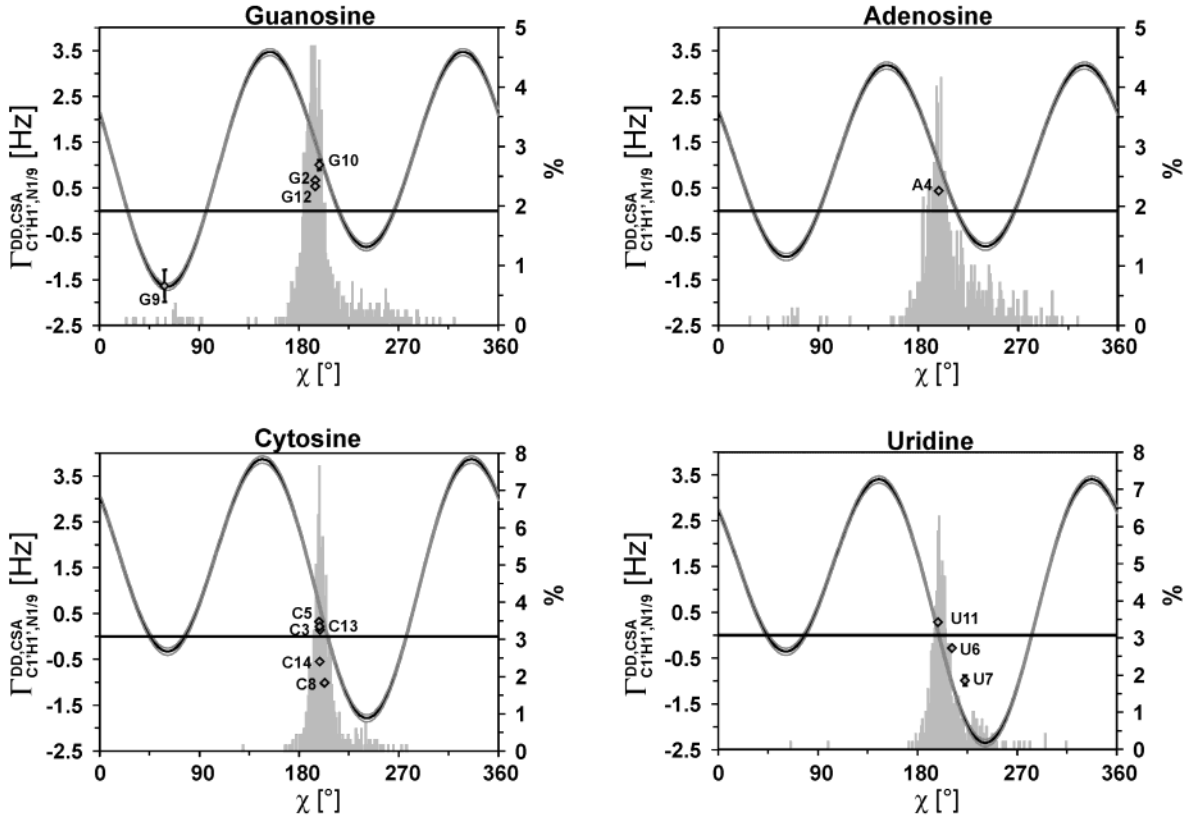

Figure 3. $\Gamma(\chi)$ for the different nucleotides. The parametrizations were calculated using a S^2 of 1, a τ_c of 2.5 ns as determined for the 14-mer RNA from R_1 and R_2 relaxation rates, and a magnetic field strength of 600 MHz. $\Gamma^{DD,CSA}_{C1'H1',N1/9}$ alone is given in black, and the additional minor contribution of $\Gamma^{DD,CSA}_{N1/9H1',C1'}$ is shown in gray. The gray bars represent the χ angle distribution in the RNA fraction of the large ribosomal subunit (PDB entry 1FFK[26]). Experimental $\Gamma^{DD,CSA}_{N1/9H1',C1'}$ rates from the 14-mer RNA are plotted against reference χ angles.

ω_N is the nitrogen Larmor frequency, γ_i is the magnetogyric ratio of the nucleus i, $r_{C1'H1'}$ is the length of the C1′H1′ dipole−dipole vector, τ_c is the rotational correlation time of the molecule, S^2 is the generalized order parameter, σ^N_{ii} is the ith component of the fully anisotropic nitrogen CS-tensor, and $\theta^{C1'H1',N1/9}_{ii}$ is the projection angles between the C1′H1′ dipole−dipole vector and the ith component of the nitrogen CS-tensor.

$\Gamma^{DD,CSA}_{C1'H1',N1/9}$ is determined from the relaxation of carbon−nitrogen double and zero quantum coherence. Among the different cross-correlated relaxation rates contributing to the relaxation of CN double and zero quantum coherence (for a detailed description, see ref 23), all dipole−dipole and CSA, CSA contributions as well as $\Gamma^{DD,CSA}_{H1'N1/9,N1/9}$ and $\Gamma^{DD,CSA}_{C1'H1',C1'}$ can be suppressed by the careful application of a train of π-pulses on the different nuclei. It is, however, experimentally not possible to separate $\Gamma^{DD,CSA}_{C1'H1',N1/9}$ from $\Gamma^{DD,CSA}_{N1/9H1',C1'}$ (Figure 1C). In contrast to $\Gamma^{DD,CSA}_{C1'H1',N1/9}$, $\Gamma^{DD,CSA}_{N1/9H1',C1'}$ is not dependent on χ. The C1′ CS-tensor is, however, sensitive to the sugar pucker mode and changes from around 30 ppm in the C3′-*endo* to about 60 ppm in the C2′-*endo* conformation.[24] Although no complete orientational information can be obtained for this tensor so far, the approximate contribution of $\Gamma^{DD,CSA}_{N1/9H1',C1'}$ to the overall rate has been calculated from the C1′ CS-tensor values and their projection angles on the C1′H1′-bond as provided in ref 25. Since this tensor displays an anisotropy of around 60 ppm, it can be used to judge the maximal possible contribution of $\Gamma^{DD,CSA}_{N1/9H1',C1'}$. For the 14-mer and the 30-mer RNA with a rotational correlation time of 2.5 and 7 ns, the maximal contribution of $\Gamma^{DD,CSA}_{N1/9H1',C1'}$ amounts to only 0.08 and 0.2 Hz, respectively.

To derive simple analytical forms of the dependence of Γ on χ, eq 1 has been expanded into the Fourier series given in Table 1. These expansions neglect the small contribution of $\Gamma^{DD,CSA}_{N1/9H1',C1'}$ discussed above. Separate parametrizations have been calculated for each nucleotide using nucleotide-specific ^{15}N CS-tensor values (Table 1; Figure 3). To obtain an estimate for the distribution of χ angles in RNA, angles extracted from the X-ray structure of the large ribosomal subunit (PDB entry 1FFK[26]) are also shown in Figure 3. In general, the angle

Table 1. Fourier Expansion of the Dependence of Γ on χ for the Different Nucleotides[a]

$$\Gamma(\chi) = 10^7\,\tau_c B_0[A_1\cos(\chi) + A_2\cos(2\chi) + A_3]$$

	A_1	A_2	A_3
adenine	0.332	−5.933	3.338
cytosine	−2.123	−7.137	4.059
guanine	1.265	−6.828	3.271
uridine	−2.908	−6.860	2.917

[a] τ_c = Overall rotation correlation time; B_0 = magnetic field strength in Tesla. The parameterization assumes isotropic diffusion as well as the absence of internal motion ($S^2 = 1$) and relies on nitrogen CS-tensor values and orientations reported for adenosine, cytosine, 2′-deoxythymine and dihydroguanosine in the solid state.[22] The N1 CS-tensor from 2′-deoxythymine has been used for uridine because no tensor for uridine is available to date.

(23) Kumar, A.; Grace, R. C. R.; Madhu, P. K. *Prog. Nucl. Magn. Reson. Spectrosc.* **2000**, *37*, 191−319.
(24) Dajaegere, A. P.; Case, D. A. *J. Phys. Chem. A* **1998**, *102*, 5280−5289.
(25) Fiala, R.; Czernek, J.; Sklenar, V. *J. Biomol. NMR* **2000**, *16*, 291−302.

distribution is much more dispersed for purines than for pyrimidines. The most populated region in all cases (~200°) coincides with a high slope in $\Gamma(\chi)$ accompanied by a sign change in the case of cytosine and uridine, indicating a high sensitivity to structural differences in this region.

Similar to $\Gamma^{DD,CSA}_{C1'H1',N1/9}$, $\Gamma^{DD,CSA}_{C2'H2',N1/9}$ (Figure 1B) is also dependent on the conformation around χ and can therefore be used as an additional parameter for angle determination. However, due to the dependence of this Γ-rate on the ribose pucker mode, it can only be applied in cases where the ribose conformation is characterized and rigid. (In the case of $\Gamma^{DD,CSA}_{C2'H2',N1/9}$, the contribution of $\Gamma^{DD,CSA}_{H2'N1/9,C2'}$ has been disregarded entirely due to the relative length of the HN dipole−dipole vector: 2.6 Å for both C3′-*endo* and C2′-*endo* conformation.)

Materials and Methods

Sample Preparation. The uniformly ^{13}C,^{15}N-labeled 14-mer RNA (5′-PO_4^--GGCAC**UUCG**GUGCC-3′; bold residues constitute the loop) was purchased from Silantes GmbH (München, Germany). The concentration of the NMR sample was 0.7 mM in 20 mM KH_2PO_4/K_2HPO_4, pH 6.4, 0.4 mM EDTA and 10% v/v D_2O. The 30-mer (5′-PO_4^--GGCACUCUGGUAU**CACG**GUACCUUUGUGUC-3′), which is selectively ^{13}C,^{15}N-labeled in the G and C residues, was synthesized by *in vitro* transcription with T7-RNA polymerase with a linearized plasmid DNA as template and purified as described previously.[27] Unlabeled rNTPs were purchased from SIGMA (Taufkirchen, Germany); labeled nucleotides were obtained from Silantes GmbH (München, Germany). The final concentration of the NMR sample was 1.2 mM in 10 mM KH_2PO_4/K_2HPO_4, pH 6.2 with 40 mM KCl, 0.2 mM EDTA, and 99.99% v/v D_2O.

NMR Spectroscopy. The NMR data were collected on a Bruker Avance 600 MHz spectrometer equipped with a 5 mm $^1H\{^{13}C/^{15}N\}$ Z-Grad TXI CryoProbe, an AV 700 MHz UltraShield instrument equipped with a 5 mm $^1H\{^{13}C/^{15}N\}$ Z-Grad TXI probe and an AV 900 MHz spectrometer with a 5 mm $^1H\{^{13}C/^{15}N\}$ XYZ-Grad TXI probe. The data were processed on a Silicon Graphics computer (Origin2000) using Bruker NMRSuite (XwinNMR 3.5 and TopSpin1.1) programs and analyzed in Felix2000 (msi). Measurements were carried out at 298 K for the 14-mer and 310 K for the 30-mer RNA.

NMR Spectroscopy: Quantitative Γ(HCN) Experiment and Γ(H2′C2′N) Experiment. The quantitative Γ(HCN) experiment (Figure 4A) is a modified HCN experiment,[25,32−36] in which C,N double- and zero-quantum coherence are excited at time point **a** and allowed to evolve for a variable delay τ_M under the influence of $\Gamma^{DD,CSA}_{H1'C1',N1/9}$ into a term, which is cosh-modulated by the Γ-rate ($4H_zC_yN_y$ cosh($\Gamma^{DD,CSA}_{H1'C1',N1/9}*\tau_M$)), and into a sinh-modulated term ($2C_xN_x$ sinh($\Gamma^{DD,CSA}_{H1'C1',N1/9}*\tau_M$)) at time point **b**.[37] Two experiments are recorded: the reference experiment, in which the cosh-modulated operator is transferred back, and the cross experiment, in which the sinh-modulated operator is selected. While selection of the reference operator is achieved in an *out-and-back* manner, the specified phases (caption of Figure 4) have to be shifted, and an additional proton−carbon recoupling period has to be added in the cross experiment. In addition, a proton 90° pulse is added in the cross experiment after τ_M to remove any operators involving protons. $\Gamma^{DD,CSA}_{H1'C1',N1/9}$ can be determined from the peak intensities in the two experiments according to eq 2:

$$\Gamma^{DD,CSA}_{H1'C1',N1/9} = -\tanh^{-1}\left(\frac{ns^{ref}\, I^{cross}}{ns^{cross}\, I^{ref}}\right) * \tau_M^{-1} \qquad (2)$$

In this equation, ns^{ref} and ns^{cross} are the number of transients and I^{ref} and I^{cross} are the peak intensities in the reference and cross experiment, respectively.

As discussed above, an alternative method for the determination of $\Gamma^{DD,CSA}_{H1'C1',N1/9}$ has been presented recently,[21] relying on a *J*-coupled approach. The quantitative approach is advantageous to the *J*-coupled one in that the latter requires the evolution of coupling, which increases the number of signals in the spectrum by a factor of 2. Especially in larger systems, spectral overlap might become the limiting factor for this method.

The CN transfer and back-transfer delays (2*T*) constitute the longest periods in the pulse sequence (76 ms). To maintain the slowly relaxing CH TROSY component during this period, the 180° proton decoupling (reference experiment) or recoupling (cross experiment) pulse during the CN back-transfer, which switches the slowly and the fast relaxing TROSY component, has to be located at the end of the fourth delay *T*. The necessity to recouple protons in the cross experiment results in evolution of the anti-TROSY component for a period Δ/2, while in the reference experiment the TROSY component evolves for the whole delay 2*T*. The loss in signal intensity due to this additional relaxation effect in the cross experiment as compared to the reference experiment was estimated from the calculation of the $\Gamma^{DD,CSA}_{C1'H1',C1'}$ using carbon CS tensor values determined by Fiala et al.,[25] and τ_c values of 2.5 ns and 7 ns for the 14-mer and the 30-mer RNA, respectively. It was found to be less than 1% and the effect was therefore neglected.

It has been shown that for the ribose moiety, HCN correlations can benefit from the use of CH multiple quantum (MQ) coherence more than from the TROSY enhancement connected to C single quantum coherence.[25,34,38] The introduction of MQ constitutes only minor changes in the pulse sequence scheme and could prove advantageous, especially for larger molecules with unfavorable relaxation behavior.

The relaxation delay τ_M was optimized for maximum signal intensity in the less sensitive cross experiment, which picks up the sinh-modulated cross operator. During τ_M, signal buildup proportional to sinh($\Gamma*\tau_M$) is counteracted by signal loss due to autocorrelated relaxation of the CN double- and zero-quantum coherence. Cross-peak intensities of representative residues showed that a τ_M of 20−30 ms is optimal for both the 14-mer and the 30-mer (Figure S1, Supporting Information).

For the 14-mer RNA, the Γ(HCN) experiment was recorded at 600 MHz (τ_M =15 ms) and 700 MHz (τ_M = 20 ms). To resolve resonance overlap, the experiments at 600 MHz were repeated using a ^{15}N detected version of the Γ(HCN) experiment as described in the caption of Figure 4. For the 30-mer RNA, data were recorded at 900 MHz with τ_M = 5 ms.

In the Γ(H2′C2′N) experiment (Figure 4B), the first INEPT module is used to create H1′C1′-antiphase magnetization. During the following delay *T*, magnetization is transferred from C1′ simultaneously to both C2′ and N1 (pyrimidines) or N9 (purines). In addition, the H1′ operator is refocused during a delay Δ. At time point **a**, the double- and zero-quantum operator $4C1'_zC2'_yN_y$ has been created. During τ_M, $\Gamma^{DD,CS}_{C2'H2',N1/9}$

(26) Ban, N.; Nissen, P.; Hansen, J.; Moore, P. B.; Steitz, T. A. *Science* **2000**, *289*, 878−879.
(27) Stoldt, M.; Wöhnert, J.; Görlach, M.; Brown, L. R. *EMBO J.* **1998**, *17*, 6377−6384.
(28) Emsley, L.; Bodenhausen, G. *J. Magn. Reson.* **1992**, *97*, 135−148.
(29) Geen, H.; Freeman, R. *J. Magn. Reson.* **1991**, *93*, 93−141.
(30) Shaka, A. J.; Barker, P. B.; Freeman, R. *J. Magn. Reson.* **1985**, *64*, 547−552.
(31) Marion, D.; Ikura, M.; Tschudin, R.; Bax, A. *J. Magn. Reson.* **1989**, *89*, 496−514.
(32) Sklenar, V.; Peterson, R. D.; Rejante, M. R.; Feigon, J. *J. Biomol. NMR* **1993**, *3*, 721−727.
(33) Farmer, B. T., II; Muller, L.; Nikonowicz, E. P.; Pardi, A. *J. Biomol. NMR* **1994**, *4*, 129−133.
(34) Marino, J. P.; Diener, J. L.; Moore, P. B.; Griesinger, C. *J. Am. Chem. Soc.* **1997**, *119*, 7361−7366.
(35) Sklenar, V.; Dieckmann, T.; Butcher, S. E.; Feigon, J. *J. Magn. Reson.* **1998**, *130*, 119−124.
(36) Brutscher, B.; Simorre, J.-P. *J. Biomol. NMR* **2001**, *21*, 367−372.
(37) Felli, I. C.; Richter, C.; Griesinger, C.; Schwalbe, H. *J. Am. Chem. Soc.* **1999**, *121*, 1956−1957.
(38) Grzesiek, S.; Bax, A. *J. Biomol. NMR* **1995**, *6*, 335−339.

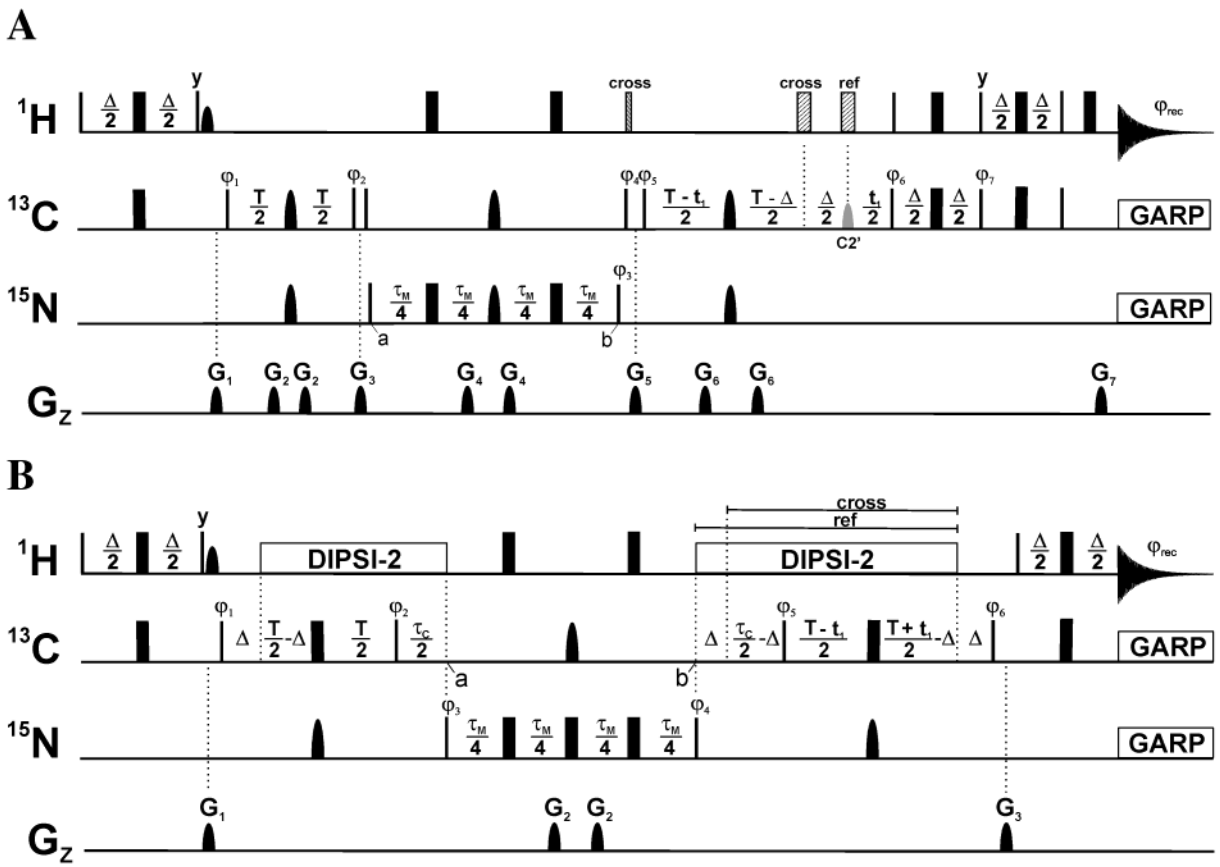

Figure 4. Quantitative Γ(HCN) experiment (A) and quantitative Γ(H2′C2′N) experiment (B). Narrow and wide bars correspond to 90 and 180° rf-pulses, respectively. Selective pulses and gradients are indicated by semi-ellipses. The default pulse phase is *x*. The pulse sequences were optimized on Bruker spectrometers with the Bruker typical phase nomenclature. An optional ^{15}N real-time evolution period can be added after τ_M. (A) The reference and the cross experiment are summarized in one pulse sequence scheme. For the reference experiment, phases φ_3 and φ_4 are set to *x*, φ_5 is set to *y*, and the hatched 180° pulse labeled "ref" is applied on protons. In the cross experiment, phases φ_3 and φ_4 are set to *y*, φ_5 is set to *x*, and the hatched 90° and 180° pulses labeled "cross" are applied. A water flipback pulse is applied after the first INEPT step. A selective off-resonant pulse on C2′ during carbon constant time chemical shift evolution is shown in gray. Acquisition parameters: Δ is equal to $1/(2*^1J_{CH})$ and set to 3.2 ms; $T = 1/(2*^1J_{CN})$ is 38 ms; τ_M is the variable $\Gamma^{DD,CSA}_{H1'C1',N1/9}$ relaxation period. The carbon offset was set to 89 ppm, and the nitrogen offset was at 158 ppm. At 600 MHz, band selective pulses were set as follows: C1′/C6,C8: 1.7 ms Q3 refocusing pulse (28); N1/N9: 1.7 ms IBURP2 inversion pulse (29); C2′: 512 μs Q3 pulse; Water flipback: 1 ms sinc pulse; Gradients: $G_1 = 1$ ms, −20 G cm^{-1}; $G_2 = 1$ ms, 20 G cm^{-1}; $G_3 = 1$ ms, −25 G cm^{-1}; $G_4 = 500$ μs, −2.5 G cm^{-1}; $G_5 = 1$ ms, 22.5 G cm^{-1}; $G_6 = 1$ ms, 20 G cm^{-1}; $G_7 = 1$ ms, 10.05 G cm^{-1}. Phase cycling: $\varphi_1 = x,(-x)$; $\varphi_2 = 4y,4(-y)$; $\varphi_3 = 8x,8(-x)$ for the reference experiment, $8y,8(-y)$ for the cross experiment; $\varphi_4 = 16x,16(-x)$ in the reference experiment, $16y,16(-y)$ in the cross experiment; $\varphi_{rec} = x,2(-x),x,(-x),2x,2(-x),2x,(-x),x,2(-x),x,(-x),2x,(-x),x,2(-x),2x,2(-x),x,(-x),2x,(-x)$. Gradient coherence selection in ω_1 is achieved by shifting phases $\varphi_6 = 2x,2(-x)$ and $\varphi_7 = 2(-y),2y$ together with changing the sign of G_6. Asynchronous GARP decoupling[30] is used to suppress heteronuclear scalar couplings during acquisition. (B) Two experiments, the reference and cross experiment, are recorded. For the reference experiment, phase φ_4 is set to *x*, and proton decoupling during the back-transfer is applied for the period labeled "ref". For the cross experiment, phase φ_4 is *y*, and protons are decoupled for the period labeled "cross". Experimental parameters: Δ is equal to $1/(2*^1J_{CH})$ and set to 3.2 ms; $T = 1/(2*^1J_{CN})$ is 38 ms; τ_M is the $\Gamma^{DD,CSA}_{H2'C2',N1/9}$ relaxation period; $\tau_c = 1/^1J_{CC} - \tau_M$. Gradients: $G_1 = 1$ ms, −20 G cm^{-1}; $G_2 = 500$ μs, 2.5 G cm^{-1}; $G_3 = 1$ ms, 40 G cm^{-1}. Phase cycling: $\varphi_1 = x,(-x)$; $\varphi_2 = 16x,16(-x)$; $\varphi_3 = 2x,2(-x)$; $\varphi_4 = 4x,4(-x)$ in the reference experiment, $\varphi_4 = 4y,4(-y)$ in the cross experiment; $\varphi_5 = 32x,32(-x)$; $\varphi_6 = 8x,8(-x)$; $\varphi_{rec} = x,2(-x),x,(-x),2x,2(-x),2x,(-x),x,2(-x),x$. In addition, φ_6 is incremented in a States-TPPI[31] manner to achieve quadrature detection in the ω_1 dimension.

is active, and this operator evolves into $4C1'_zC2'_yN_y \cosh(\Gamma^{DD,CSA}_{C2'H2',N1/9}*\tau_M)$ and $8H2'_zC1'_zC2'_xN_x \sinh(\Gamma^{DD,CSA}_{C2'H2',N1/9}*\tau_M)$ at time point **b**. To transfer the latter operator back in the cross experiment, H2′ proton magnetization is refocused during an additional delay Δ after **b**, while the reference operator is transferred *out-and-back*. Scalar interactions between C2′ and both C1′ and C3′ are suppressed by setting the total period in which C2′ is transversal to 25 ms ($\tau_M + \tau_C = 1/^1J_{CC}$). Extraction of $\Gamma^{DD,CS}_{H2'C2',N1/9}$ is similar to the quantitative Γ(HCN) experiment. The (C2′H2′,N) experiment was recorded at 600 MHz using a τ_M of 5 ms.

Results

Glycosidic Torsion Angles in the 14-mer and the 30-mer RNA. The 14-mer RNA (Figure 2A) was selected as a model compound to evaluate the accuracy of χ angle determination from the Γ(HCN) experiment, since it is conformationally rigid and contains both canonical stem regions with a low divergence in χ and a noncanonical cUUCGg tetraloop, exhibiting a broader distribution of χ angles. In addition, the tetraloop comprises an unusual U:G^{syn} base pair; all other residues adopt the *anti* conformation. Homonuclear ^3J-coupling constants indicate that the ribose moieties of all residues are fixed in one conformation (data not shown). Although there is no structure available of the 14-mer to date, the structure of cUUCGg-tetraloops has been consistently characterized by both NMR (PDB entry 1HLX[39]) and X-ray crystallography (PDB entry 1F7Y[40]). Reference χ angles (Table 2) for our investigation have been extracted as described in Table 2.

(39) Allain, F. H.; Varani, G. *J. Mol. Biol.* **1995**, *250*, 333−353.
(40) Ennifar, E.; Nikulin, A.; Tishchenko, S.; Serganov, A.; Nevskaya, N.; Garber, M.; Ehresmann, B.; Ehresmann, C.; Nikonov, S.; Dumas, P. *J. Mol. Biol.* **2000**, *304*, 35−42.

Table 2. $\Gamma^{DD,CSA}_{C1'H1',N1/9}$ and Resulting χ Angles of the 14-mer RNA Compared to the Angles from the Crystal Structure ("reference") and from the Interpretation of ^3J(C,H)-Coupling Constants ("^3J(C,H)")[a]

residue	$\Gamma^{DD,CSA}_{H1'C1',N1/9}$ [Hz]	χ [deg]		
		$\Gamma^{DD,CSA}_{H1'C1',N1/9}$	^3J(C,H)	reference
G1				194.8 ± 4.4
G2	−0.67 ± 0.04	205 ± 1	192 ± 2	194.8 ± 4.4
C3	−0.14 ± 0.01	203 ± 1		198.4 ± 3.1
A4	−0.44 ± 0.01	207 ± 1	198.5 ± 1.5	198.2 ± 3.5
C5	−0.32 ± 0.07	201 ± 1	191 ± 8	197.9
U6	0.29*	221	196.5 ± 4.5	211
U7	0.99 ± 0.11	209 ± 4	217.5 ± 9.5	223
C8	1.03 ± 0.08	218 ± 2	210.5 ± 6.5	202.6
G9	1.64 ± 0.35	57 ± 19	44 ± 4	58.7
G10	−1.00 ± 0.11	201 ± 2	215.5 ± 13.5	198.3
U11	−0.29*	195		198.2 ± 3.0
G12	−0.53 ± 0.04	207 ± 1	192 ± 4	194.8 ± 4.4
C13	−0.21 ± 0.04	202 ± 1	189.5 ± 3.5	198.4 ± 3.1
C14	0.55 ± 0.08	211 ± 1	198 ± 5	198.4 ± 4.4
RMSD [deg]	$\Gamma^{DD,CS}_{H1'C1',N1/9}$		14.1	6.3
	^3J(C,H)	14.1		7.8

[a] The averaged Γ-rates from measurements at 600 and at 700 MHz are given. Γ-rates measured at the two fields are listed separately in Table S1 in the Supporting Information. ^3J(C,H)-coupling constants have been determined and analyzed by a refined, nucleotide-type specific Karplus-relation as described previously.[8−10] The averaged χ angles from the analysis of ^3J(C2/4,H1′) and ^3J(C6/8,H1′) are given. Errors for Γ-rates are calculated from multiple measurements at different τ_M evolution periods and different magnetic fields (see Materials and Methods). For data labeled with an asterisk no error is given, since they were obtained only once. The reference angles have been extracted from the crystal structure (PDB entry 1HLX) for residues 5 to 10. For the remaining residues a canonical conformation has been found. Therefore, base type specific mean χ angle values calculated from an A-form RNA crystal structure at high resolution (PDB entry 1QC0) and their standard deviations have been used for these residues. Errors for coupling constant-derived χ angles have been taken from the differences between angle determination from ^3J(C2/4,H1′) and from ^3J(C6/8,H1′). For both Γ-rates and *J*-couplings, only the χ angles closest to the reference values have been extracted from the degenerate parametrization curves.

The 30-mer RNA (Figure 2B; PDB entry 1RFR[41]) consists of two canonical A-form stem regions connected by three pyrimidine mismatch base pairs (U:U, C:U, U:U) and a uCACGg tetraloop, which has been shown by NMR[41] to adopt a structure similar to the one of the cUUCGg tetraloop. The loop contains an unusual C:G^{syn} base pair. As in the 14-mer, all residues are rigid. The χ angles from the NMR structure are summarized in Table S2 (Supporting Information).

χ Angle Determination from $\Gamma^{DD,CSA}_{H1'C1',N1/9}$. Figure 5 shows the reference (Figure 5A) and the cross spectra (Figure 5B) of the quantitative Γ(HCN) experiment applied to the 14-mer RNA. $\Gamma^{DD,CS}_{H1'C1',N1/9}$ rates have been extracted from the peak intensities in the two different experiments as described in Materials and Methods.

$\Gamma^{DD,CSA}_{H1'C1',N1/9}$ obtained on the 14-mer RNA are listed in Table 2 together with the χ angles extracted using the Γ(χ) correlations given in Table 1. The precision of Γ-rate measurement is 0.1 Hz as determined from the mean deviation of the Γ-rates for all residues from multiple measurements at different field strengths and different relaxation delays τ_M (see Materials and Methods).

Figure 6 shows the correlation of the χ angles derived from $\Gamma^{DD,CS}_{H1'C1'N1/9}$ with the reference angles from the X-ray structure of the 14-mer (Table 2). The $RMSD_{\Gamma(HCN)/X\text{-}ray}$ is 6.3°. This agreement compares to the one between the reference angles and χ angles derived from the analysis of ^3J(C2/4,H1′)- and ^3J(C6/8,H1′)-coupling constants, which are also given in Table 2 ($RMSD^{3}_{J(C,H)/X\text{-}ray}$ = 7.8°). The agreement between the *J*-coupling and the cross-correlated relaxation-derived χ angles is slightly worse ($RMSD^{3}_{J(C,H)/\Gamma(HCN)}$ = 14.1°). These results show that in the case of a rigid molecule such as the 14-mer RNA, the Γ(χ) correlations presented here are applicable. Hence, the transfer of ^{15}N CS-tensor information obtained in the solid state on model compounds to oligonucleotides in solution is valid.

As shown in Figure 3, due to a high slope and a sign change in this region, $\Gamma^{DD,CS}_{C1'H1',N1/9}$ is especially sensitive for χ angles in the *anti* region of around 140−220°, which is the most populated region in the ribosome reference structure (see Figure 3). Sensitivity to χ angles in the *syn* region is lower.

For the 30-mer RNA, the accuracy of χ angle determination is 9.3° compared to the χ angles from the NMR structure.[41] The sensitivity is sufficient at a 900 MHz spectrometer using 1024 transients per t_1-increment. The cross and reference spectra are shown in Figure 5C and Figure 5D, and the measured Γ-rates and ^3J(C,H)-coupling constants as well as the resulting χ angles are summarized in Table S2 in the Supporting Information. Since the overall RMSD in the case of the more anisotropic 30-mer RNA is of the same order of magnitude as the RMSD of the 14-mer RNA, we conclude that the effect of diffusion anisotropy is not significant and can be safely neglected in the size range of up to around 30 nucleotides. This finding is in agreement with the results on a 36-mer.[21]

$\Gamma^{DD,CSA}_{C2'H2',N1/9}$ for Resolving χ Angle Ambiguities. Similar to the angle ambiguity resulting from the interpretation of ^3J-coupling constants, angle determination from cross-correlated relaxation rates is up to 4-fold degenerate. In the case of C2′-*endo*, but not in the case of C3′-*endo* ribose puckering, the additional determination of $\Gamma^{DD,CS}_{C2'H2',N1/9}$ as a second, independent parameter allows the removal of the angle ambiguity resulting from the interpretation of $\Gamma^{DD,CSA}_{C1'H1',N1/9}$ alone. $\Gamma^{DD,CSA}_{C2'H2',N1/9}$ is obtained from an adjusted Γ(HCN) experiment (Figure 4B), the Γ(H2′C2′N) experiment. The parametrization and the experimental values for both $\Gamma^{DD,CSA}_{C2'H2',N1}$ and $\Gamma^{DD,CSA}_{C1'H1',N1}$ are shown

(41) Ohlenschläger, O.; Wöhnert, J.; Bucci, E.; Seitz, S.; Häfner, S.; Ramachandran, R.; Zell, R.; Görlach, M. *Structure*, in press.

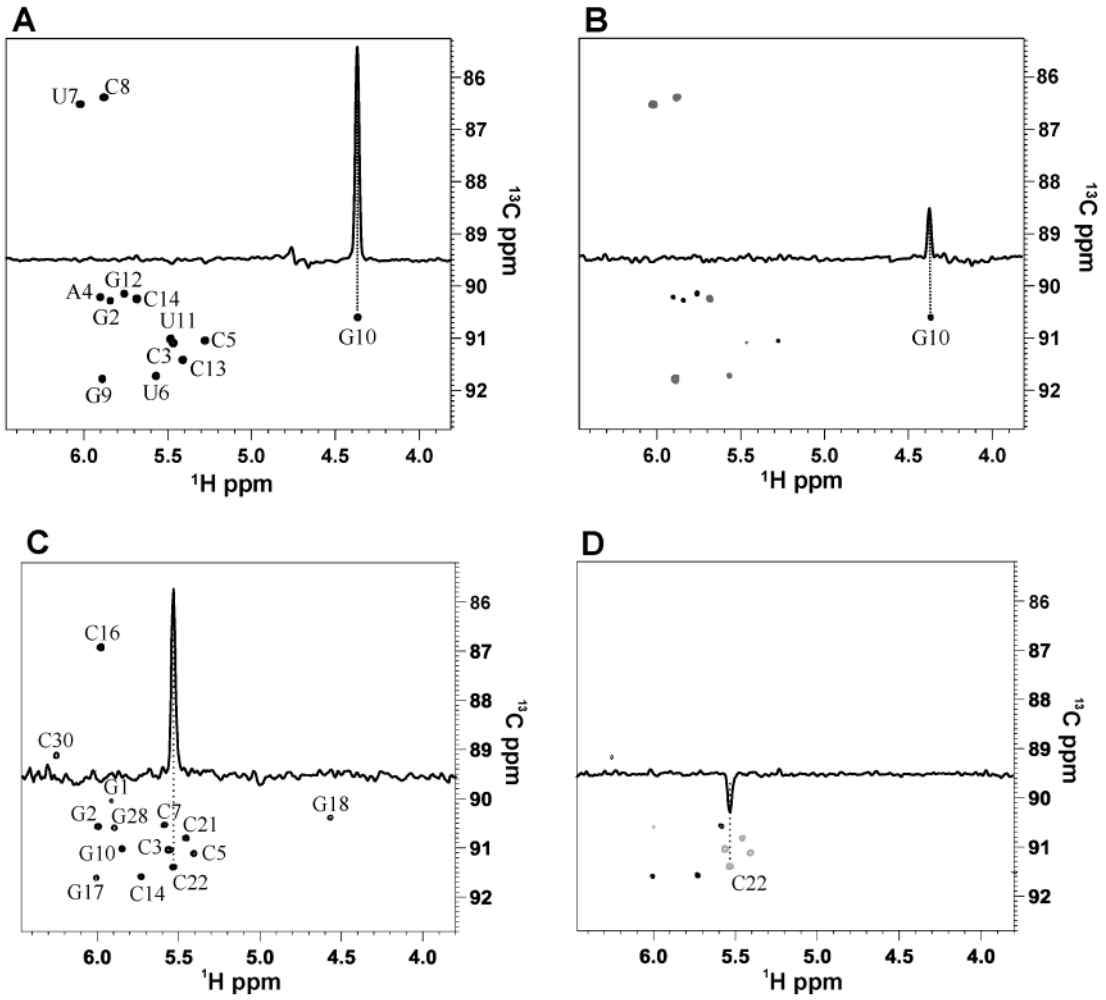

Figure 5. Γ(HCN) spectra of the 14-mer (A and B) and the 30-mer RNA (C and D). (A,C) Reference experiments. (B,D) Cross experiments. Resonance assignments are given. The spectra of the 14-mer were recorded on a 700 MHz spectrometer, and the spectra of the 30-mer were obtained on a 900 MHz spectrometer. τ_M was set to 15 ms (5 ms) for the 14-mer (30-mer). For both molecules, the reference experiment was obtained with 32 and the cross experiment with 1024 transients. The overall duration of the two experiments was about 15 h.

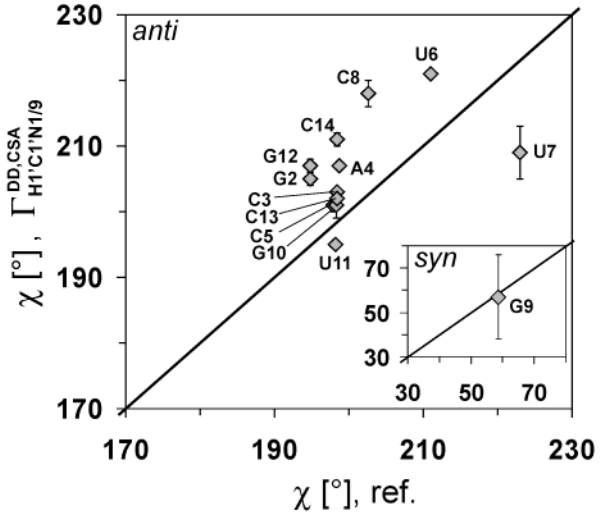

Figure 6. χ angles resulting from the analysis of $\Gamma^{DD,CSA}_{H1'C1',N1/9}$ for the 14-mer RNA plotted against the reference χ angles. The data for G9 in the *syn* conformation are shown in the insert.

in Figure 7 for U7 and C8, the two residues in the 14-mer RNA, which are in C2′-*endo* conformation. Whereas both Γ-rates alone result in two possibilities for χ, the actual value for χ can be selected by virtue of the agreement between the χ values from $\Gamma^{DD,CSA}_{C1'H1',N1}$ and $\Gamma^{DD,CS}_{C2'H2',N1}$ (gray circles in Figure 7).

Incorporation of $\Gamma^{DD,CSA}_{H1'C1',N1/9}$ into RNA Structure Calculations. In conventional RNA structure determination by NMR, the glycosidic bond angle χ is restricted to either *syn* or *anti* from the analysis of the H6/8−H1′ NOE. χ angle restraints determined from the measurement of $\Gamma^{DD,CSA}_{H1'C1',N1/9}$ offer a way to incorporate more direct torsion angle information into the structure calculation. In addition, while extraction of the Γ-rates constitutes a linear task, in the case of NOE information, both of the involved protons have to be identified, thus increasing the complexity of the process. For the structure calculation on the 30-mer RNA,[41] an exceptionally large set of NOEs has been used (~27 NOEs per residue), resulting in a very well-defined structure (RMSD 0.67 Å for all heavy atoms). The χ angles from this structure have been used here to assess the accuracy of the Γ(HCN) experiment.

To evaluate the structural relevance of the χ angle restraints derived from $\Gamma^{DD,CSA}_{H1'C1',N1/9}$, we have incorporated them into a Distance Geometry/Simulated Annealing structure calculation in torsion angle space using the program CYANA.[42] For

(42) Güntert, P.; Mumenthaler, C.; Wüthrich, K. *J. Mol. Biol.* **1997**, *273*, 283−298.

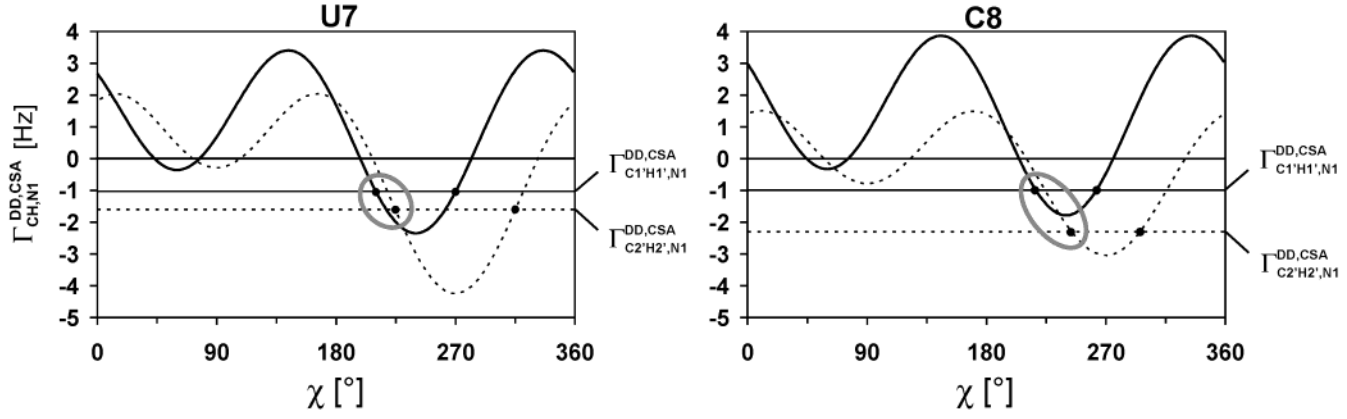

Figure 7. $\Gamma^{DD,CSA}_{C1'H1',N1}$ (solid line) and $\Gamma^{DD,CSA}_{C2'H2',N1}$ (dashed line) for the residues U7 (left) and C8 (right) of the 14-mer RNA. Possible χ angle values for the measured $\Gamma^{DD,CSA}_{CH,N1}$ values are shown by black dots. The regions in which the actual χ angle is located are indicated by gray circles.

comparison, a second calculation comprising only a minimal set of easily accessible NOE restraints (with the exception of NOEs involving the H5′/H5″ protons, all intraresidual sugar-to-base and sugar-to-sugar NOEs (225 in total) were removed) was performed. The Γ-rate-derived restraints are directly incorporated as χ angles with a variation of 10°. All possible angles from the parametrization are considered.

Inclusion of the $\Gamma^{DD,CS}_{C1'H1',N1/9}$-derived χ angle restraints results in a decrease of the mean RMSD from 6.9 to 2.6° for residues G2, C3, G5, G7, C14, C21, G28, and G30 (Figure 8). For G17, which is in the *syn* conformation, the NOE-based structure calculation results in a χ angle of 67.5 ± 3.8°. Upon incorporation of the Γ-rate derived angle restraints, two χ angles become possible, 42.8° and 79.6°, signifying that in this angle region NOE and Γ-rate data are not sufficient to discriminate between the two possible angles derived from the Γ-rates.

Conclusions

In conclusion, we have introduced two new NMR experiments for the determination of the glycosidic bond angle χ in oligonucleotides from the angular dependence of CH-dipolar, N-CSA cross-correlated relaxation rates ($\Gamma^{DD,CSA}_{C1'H1',N1/9}$ and $\Gamma^{DD,CSA}_{C2'H2',N1/9}$). In the case of $\Gamma^{DD,CS}_{C1'H1',N1/9}$, we have provided Γ(χ) parametrizations for each nucleotide based on ^{15}N tensor values obtained on model compounds in the solid state. Application to a 14-mer RNA of known structure has shown that by the virtue of these parametrizations, χ can be determined with an accuracy of about 10°.

Data interpretation, however, relies on detailed knowledge of the nitrogen CS-tensors in the nucleobases. To date, only one complete study of these tensors in model compounds (mononucleoside crystals) is available.[22] All of these model compounds are in the *anti* conformation. With regard to a possible dependence of the CS-tensor on conformation, the method proposed here will clearly benefit from a direct, residue-specific determination of the nitrogen CS-tensor in oligonucleotides in solution. In principle, the fully anisotropic ^{15}N CS-tensor can be determined from the geometric information conveyed in multiple cross-correlated relaxation rates correlating the N CS-tensor to the different neighboring dipole−dipole vectors or from the anisotropic chemical shift information extracted from samples in different alignment media. For proteins, a number of studies have been carried out along these lines aiming at the determination of the amide ^{15}N CS-tensor in solution.[43−45] Although these methods assume a number of simplifications such as the axial symmetry of the CS-tensor or a common tensor value for all sites, they could be expanded to the site-specific determination of the fully anisotropic CS-tensor of N9 and N1 in oligonucleotides.

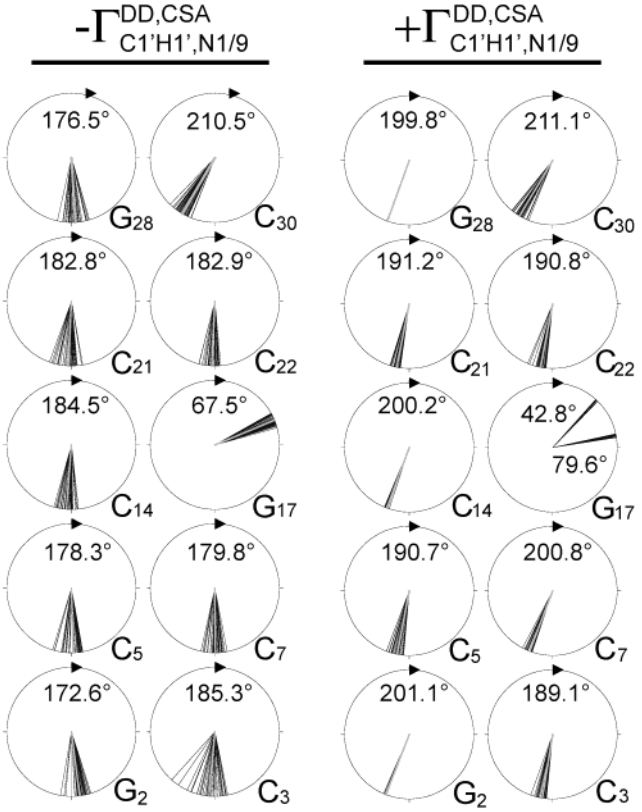

Figure 8. Results of the CYANA structure calculations on the 30-mer RNA. Left: χ angle distributions of the relevant residues resulting from the structure calculation including a minimal set of NOE values (see text). Right: χ angle distributions of the relevant residues resulting from the structure calculation including a minimal set of NOE values and χ angle restraints from the analysis of $\Gamma^{DD,CSA}_{C1'H1',N1/9}$. In both cases, χ angles from the 40 structures with the lowest target function values from the calculated ensemble of 200 structures are shown.

(43) Tjandra, N.; Szabo, A.; Bax, A. *J. Am. Chem. Soc.* **1996**, *118*, 6986−6991.
(44) Fushman, D.; Cowburn, D. *J. Am. Chem. Soc.* **1998**, *120*, 7109−7110.
(45) Boyd, J.; Redfield, C. *J. Am. Chem. Soc.* **1999**, *121*, 7441−7442.

Despite the need for more detailed studies on the nitrogen CS-tensor in solution, we have shown that the quantitative Γ(HCN) experiment can be used to determine χ with an accuracy equivalent to the one of ^3J(C,H) scalar coupling constants. The Γ(H2′C2′N) experiment offers a means to remove the ambiguity in angle determination from $\Gamma^{DD,CSA}_{H1'C1',N1/9}$ in favorable cases. Due to the linear dependence of $\Gamma^{DD,CSA}_{H1'C1',N1/9}$ on both the magnetic field strength and the overall correlation time τ_c, the Γ(HCN) experiment is an interesting method for application to larger systems. It has been successfully applied to a sizable RNA of 30 nucleotides without severe loss in sensitivity. In the case of conformational averaging, however, χ cannot be extracted from $\Gamma^{DD,CSA}_{H1'C1',N1/9}$ without detailed dynamical information.

Acknowledgment. We thank Boris Fürtig for providing the assignment of the 14-mer RNA and Jonas Noeske and Ulrich Schieborr for data evaluation. We appreciate the support of Dirk Stueber and David Grant concerning the ^{15}N chemical shift tensors. We are grateful to Elke Stirnal and Sabine Häfner for help in the 30-mer RNA sample preparation.

Supporting Information Available: Figure showing the dependence of the peak intensities in the cross experiment on the mixing time τ_M for the 14-mer and the 30-mer RNA. Appendix explaining the origin of the reference χ angles for the 14-mer RNA with a table containing $\Gamma^{DD,CSA}_{H1'C1',N1/9}$ and resulting χ angles for the 14-mer RNA in dependence of the magnetic field strength and a table containing $\Gamma^{DD,CSA}_{H1'C1'N1/9}$ and resulting χ angles compared to χ angles from the NMR structure and the analysis of ^3J-coupling constants (PDF). This material is available free of charge via the Internet at http://pubs.acs.org.

JA0367041